www.ijmer.com Vol.1, Issue.2, pp-430-442 ISSN: 2249-6645

Study on the influence of spray parameters of Ar-N_2 Plasma spray process using CFD analysis

Mr. Mohammed Yunus[1], Dr. J. Fazlur Rahman[2]
[1]Research scholar, Anna University of Technology, Coimbatore,
Assistant Professor, Department of Mechanical Engineering
H.K.B.K.C.E. Bangalore
[2]Professor Emeritus, Department of Mechanical Engineering
H.K.B.K.C.E. Bangalore,

ABSTRACT

Thermal sprayed surface coatings are extensively used for a wide range of industrial applications. In the plasma spray process used in thermal spraying, the temperature of substrate and conduction of heat along the thickness of ceramic oxide coatings (TCOC) play an important role in the bond strength and microstructure of the coatings, which decides its performance and quality. In this study, using Ansys-CFX, a 3D numerical model is developed to study heat exchange between plasma jet and substrate and along the TCOC to predict life of the coating. The plasma jet temperature, velocity distribution and heat exchange to the substrate surface and coatings have been thoroughly analyzed for the effects of various spray parameters (SP) such as gas composition, standoff distances (sod), velocity and temperature of a jet. It is found that 3D modeling has shown promising results on substrate heating. The effect of spray parameters could also be assessed and validated by comparing with experimental results.

Keywords **- Computational Fluid Dynamics, heat flux, spray process, Numerical modeling, Partially Stabilized Zirconia, Temperature and velocity distribution Zirconia Toughened Alumina.**

1. INTRODUCTION

In ceramic oxide coatings, an atmospheric plasma spraying process (APS) is widely used. Plasma spraying has been extensively used in various

industrial components for producing different kinds of coatings, such as wear, corrosion, pitting and thermal resistance coatings [1], [3-4]. In this technique, plasma gas which is a high temperature ionized gas. When a strong electric arc is struck between tungsten electrode (cathode) and a nozzle (anode) in the presence of Argon and nitrogen/ hydrogen mixture in the chamber, the gas gets ionized which called plasma is reaching the temperature of the order of 14,000^{0}C to 20,000^{0}C. Injected particles of coating materials are heated inside the plasma jet and molten droplets are projected on the substrate with high velocities to form the coating.

The properties of the resulting layers are strongly depend on how large particle's velocity, temperature and melting degree are at the moment of impinging on the substrate[2],[5],[7]. Therefore, the manufacturing process requires the adjusting of a large number of parameters to get a good quality of coating (to suit our functional requirement) and for life and quality prediction of coating. Some of the parameters are

1. Flow rate, Gas composition, velocity and temperature of the plasma, substrate heating, type of coatings, standoff distance (distance between nozzle and substrate), size of the powder particles.
2. Conduction of heat in different types of coatings.

It is impossible in practice to determine the respective influence of all these single factors, on the resulting thermal barrier coating. Thus an accurate modeling of the whole plasma spraying process provides us with a powerful tool to understand better, the process and to determine the optimal conditions for the TBC production.

Much work has been done to study the effect of above parameters in the plasma jet without considering the presence of coating surface with substrate condition, using two and three-dimensional analysis [2],[7], [9]& [15-18]. It is found that the presence of coated substrate has major effect on these parameters. In order to ascertain its effect, the present study, based on numerical modeling analysis, has been done and the effect of various parameters have been discussed from the point of view of good quality coating.

Three different commercially available ceramic coatings powders namely, Partially Stabilized Zirconia (PSZ), Zirconia toughened alumina (ZTA consist of 80% alumina and 20% PSZ) and Super-Z alloy (20% alumina and 80% PSZ) were used for the coatings [1], [3] and [19].

1.1 Modeling approach

To simulate the plasma jet, it is assumed that plasma is in steady state, in local thermo-dynamical equilibrium, optically thin, Incompressible, turbulent and mass diffusivity is equal to thermal diffusivity [15-17]. The plasma jet is impinged on pre heated substrate (between 27^0C to 200^0C) in an open atmosphere and plasma gas used is a mixture of argon and nitrogen. To increase the enthalpy and thermal conductivity of the plasma jet, usually a small amount of nitrogen is added to argon [6-7] &[12]. Twelve different computational geometries are created for this study. Figure 1.(a), (b), (c), (d),(e), (f) respectively, shows computational domains for torch to substrate distances, 0.08, 0.1, 0.11, 0.14 and 0.15 m. These geometries are created using Ansys ICEM CFD10.0. The mesh is refined at core region of the jet to treat the large temperature and velocity gradients both in axial and in radial directions [7] & [9]. The nozzle exit diameter is 0.007 m. The Ansys-CFX 11.0 has been used for preprocessing, solving and post processing of results.

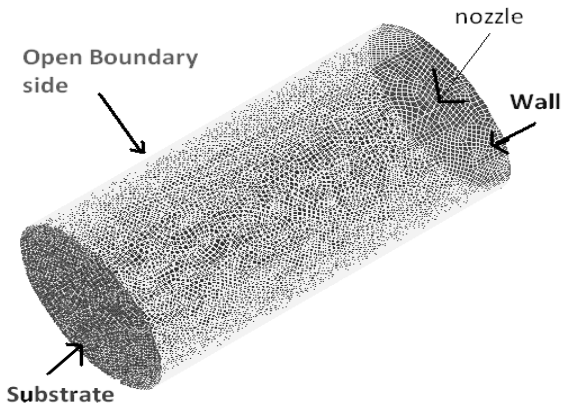

Figure 1. Computational geometry simulates the plasma jet with substrate at a standoff distance of 0.08m.

Figure 2. Computational geometry simulates the plasma jet with substrate at a standoff distance of 0.1m.

Figure 3. Computational geometry simulates the plasma jet with substrate at a standoff distance of 0.11m.

Figure 4. Computational geometry simulates the plasma jet with substrate at a standoff distance of 0.14m.

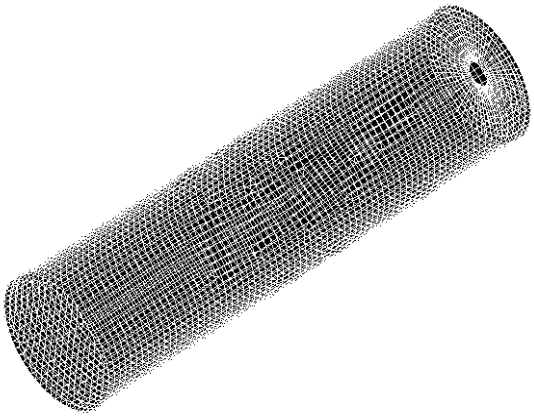

www.ijmer.com Vol.1, Issue.2, pp-430-442 ISSN: 2249-6645

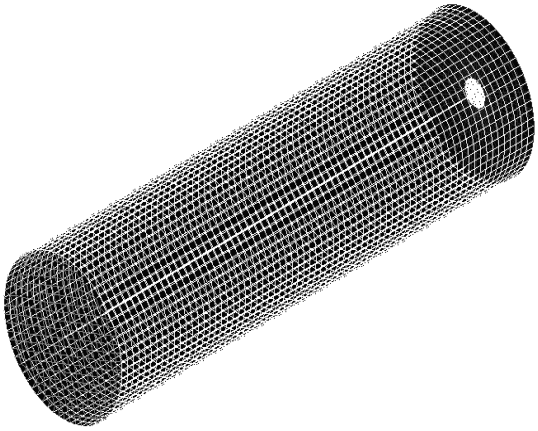

Figure 5. Computational geometry simulates the plasma jet with substrate at a standoff distance of 0.15m.

2. Results and Discussion

Analysis carried out for 16 kW plasma spray torch chosen to simulate the nozzle exit temperature and velocity profiles have been used to prepare different kinds of coatings such as Partial stabilized zirconia (PSZ), Super-Z and Zirconia Toughened Alumina (ZTA).

It is clear from this result that effect of nitrogen content in the plasma gas on torch power and efficiency is stronger than that of the argon gas flow rate. Hence, temperature and velocity of the plasma jet decrease with increasing argon gas flow rate. The similar effect has been seen for other stand-off distances.

The gas flow rates of both argon and nitrogen are fixed at three different values percentages of Ar90%, $N_2$10%, Ar 75%, N_2 25% and Ar50%, $N_2$50% respectively. The total heat flux to the substrate increases with increasing flow rate. The similar effect has been observed at stand-off distances of 0.1 and 0.125 m.

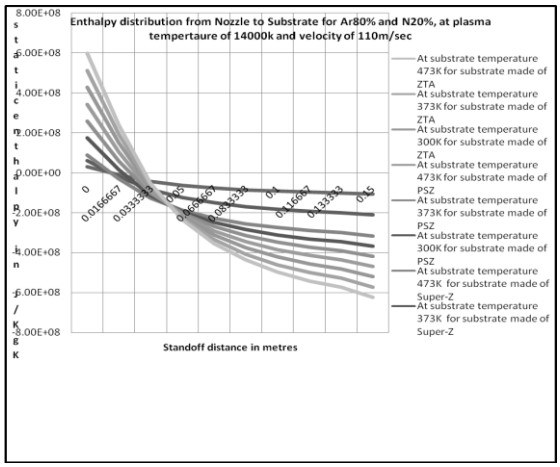

Fig.6.a. Enthalpy distribution for sod =0.15m at 110m/sec.

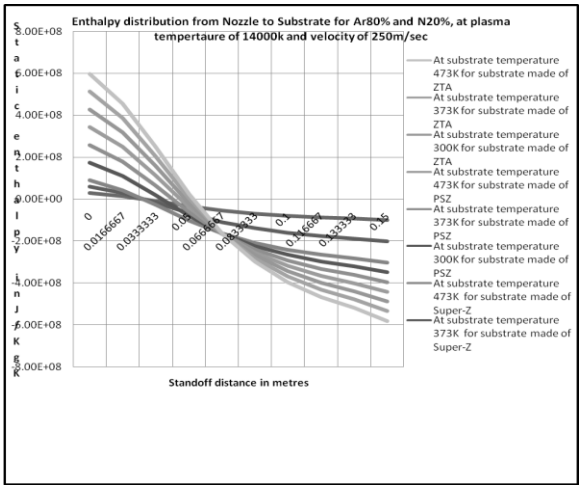

Fig.6.b. Enthalpy distribution for sod =0.15m at 250m/sec.

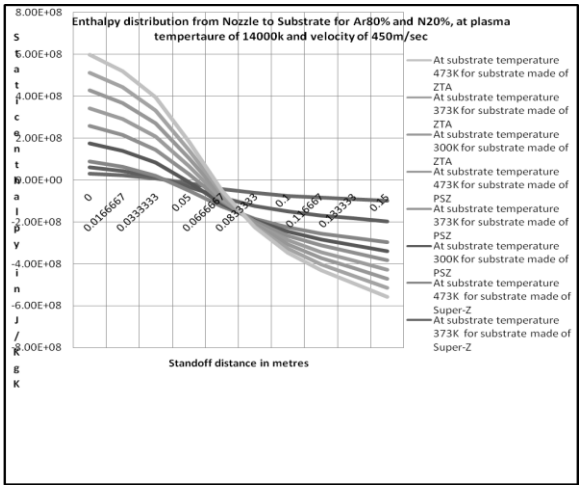

Fig.6.c. Enthalpy distribution for sod =0.15m at 450m/sec.

www.ijmer.com Vol.1, Issue.2, pp-430-442 ISSN: 2249-6645

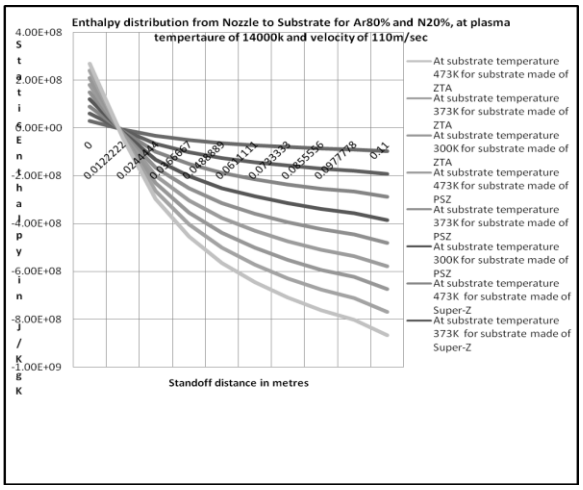

Fig.6.d. Enthalpy distribution for sod =0.11m at 110m/sec.

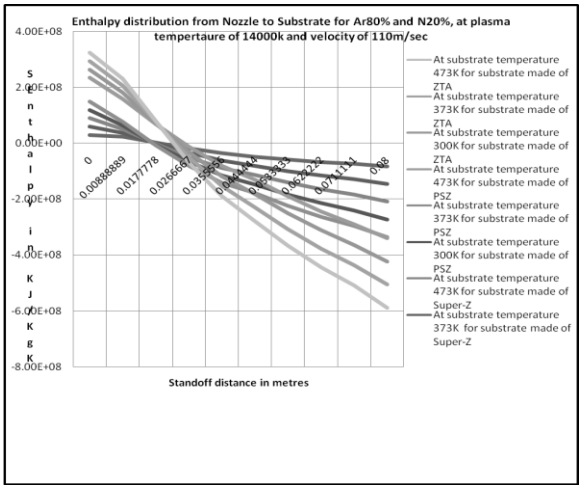

Fig.6.e. Enthalpy distribution for sod =0.08m at 110m/sec.

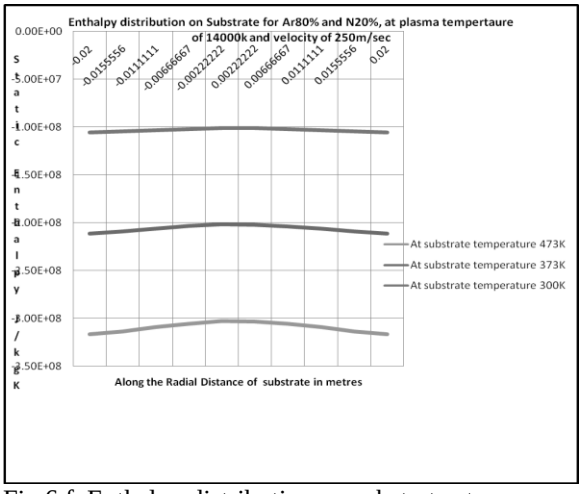

Fig.6.f. Enthalpy distribution on substrate at 250m/sec.

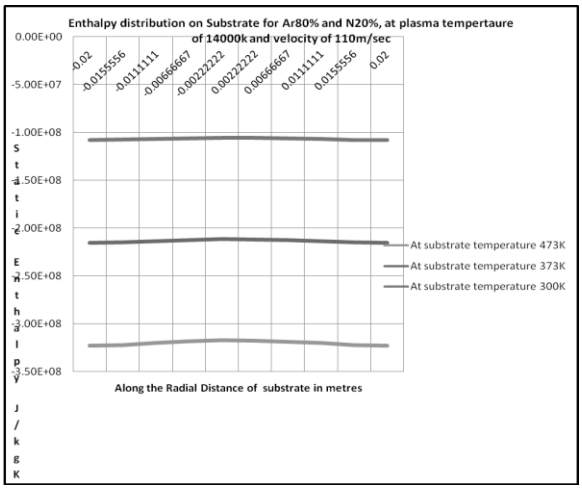

Fig.7.a. Enthalpy on substrate in radial direction at 110m/sec and sod = 80mm.

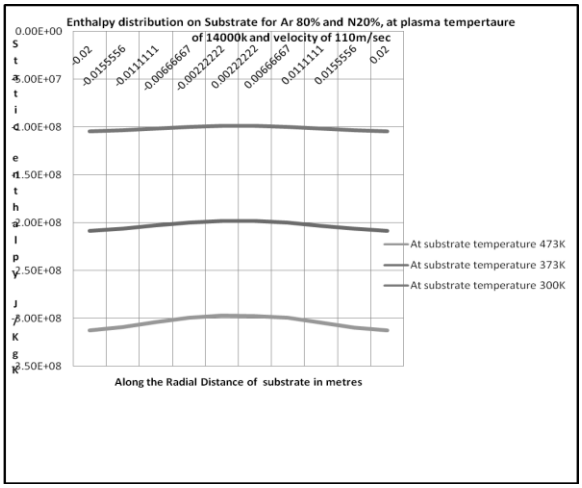

Fig.7.b. Enthalpy on substrate in radial direction at 110m/sec and sod = 100mm.

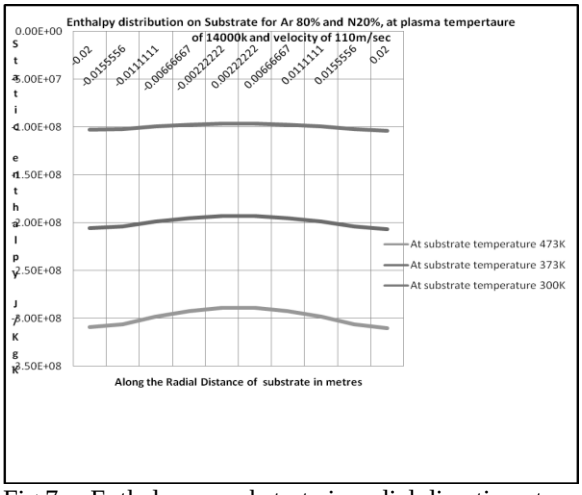

Fig.7.c. Enthalpy on substrate in radial direction at 110m/sec and sod = 110mm.

www.ijmer.com Vol.1, Issue.2, pp-430-442 ISSN: 2249-6645

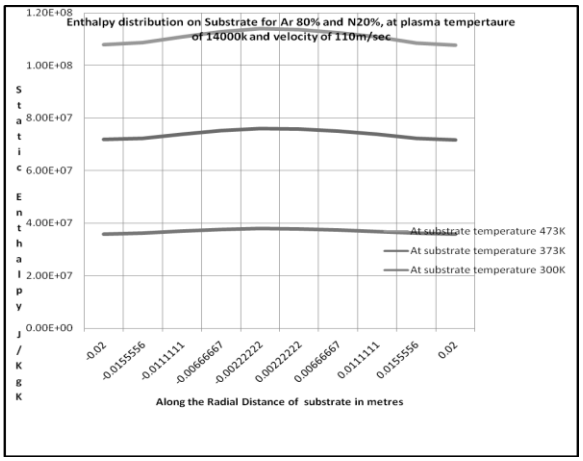

Fig.7.d. Enthalpy on substrate in radial direction at 110m/sec and sod = 140mm.

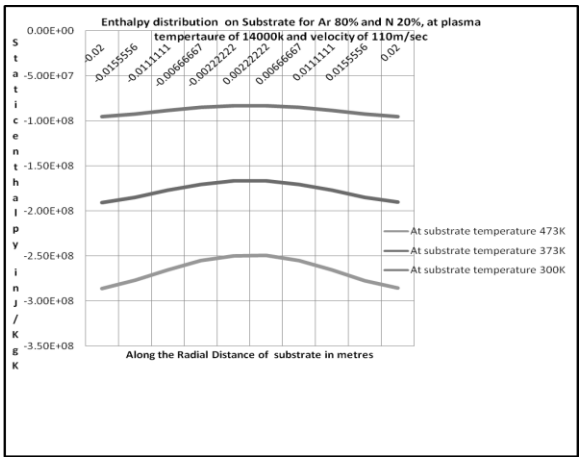

Fig.7.e. Enthalpy on substrate in radial direction at 110m/sec and sod = 150mm.

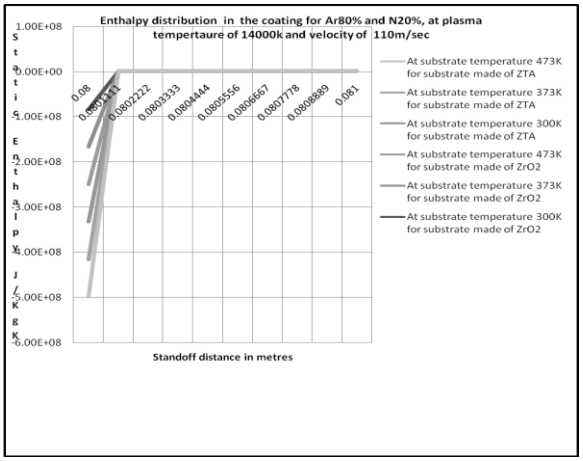

Fig.8.a. Enthalpy along coating thickness at 110m/sec and sod = 100mm.

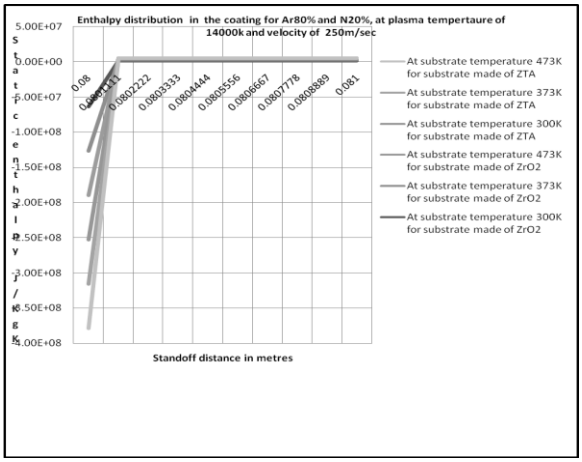

Fig.8.b. Enthalpy along coating thickness at 250m/sec and sod = 80mm.

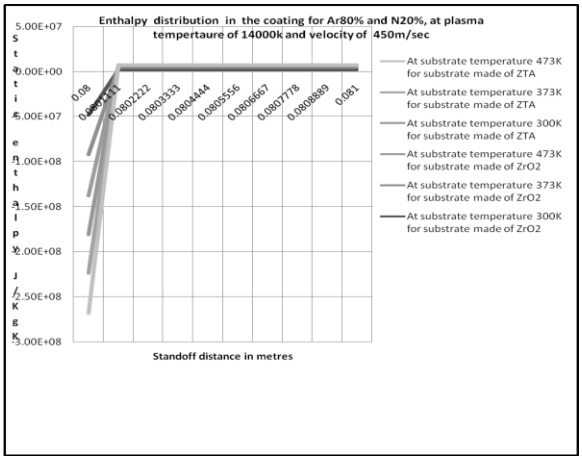

Fig.8.c. Enthalpy along coating thickness at 450m/sec and sod = 80mm.

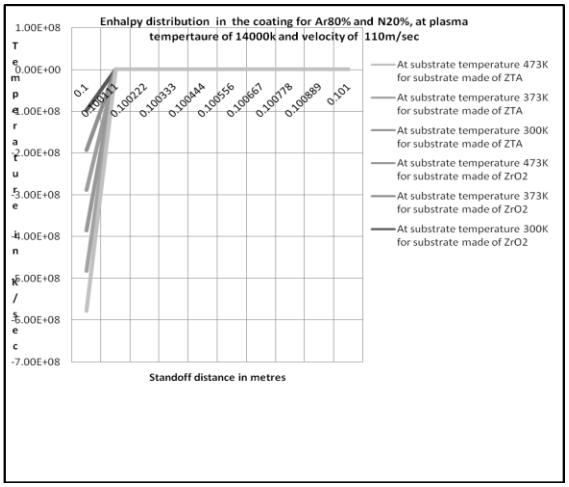

Fig.8.d. Enthalpy along coating thickness at 110m/secandsod=100mm.

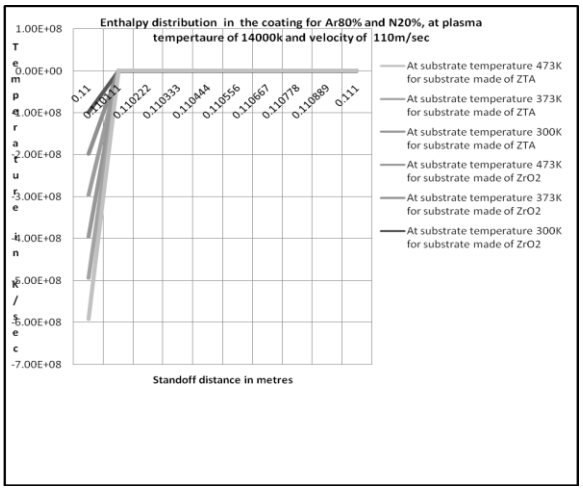

Fig.8.e. Enthalpy along coating thickness at 110m/sec and sod = 110mm

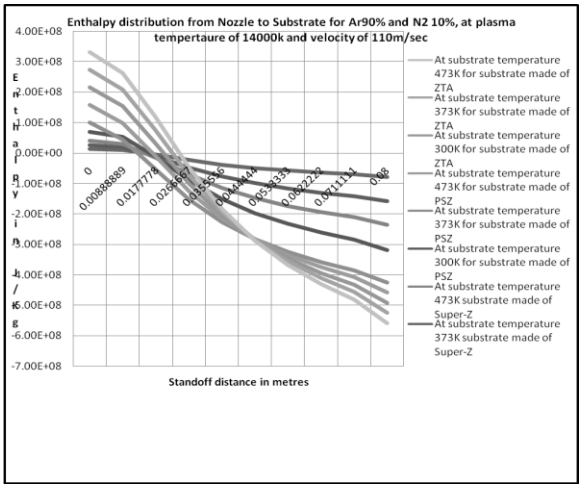

Fig.9.a. Enthalpy distribution for sod =0.08 m at 110 m/sec and Ar90%+$N_2$10%.

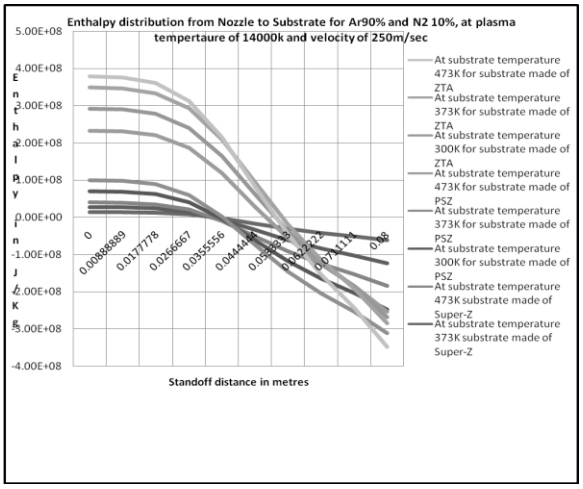

Fig.9.b. Enthalpy distribution for sod =0.08m at 250 m/sec and Ar90%+$N_2$10%.

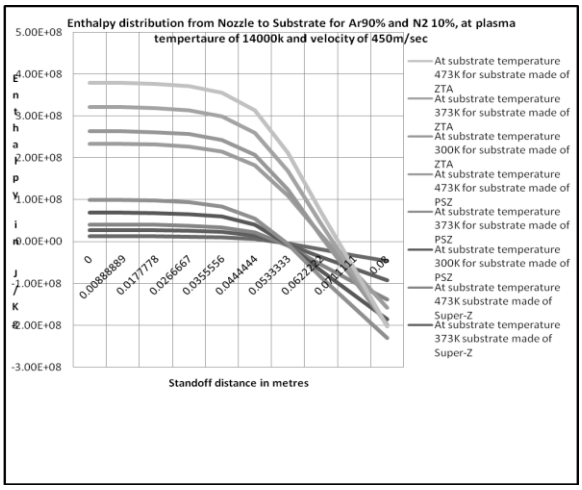

Fig.9.c. Enthalpy distribution for sod =0.08m at 450 m/sec and Ar90%+$N_2$10%.

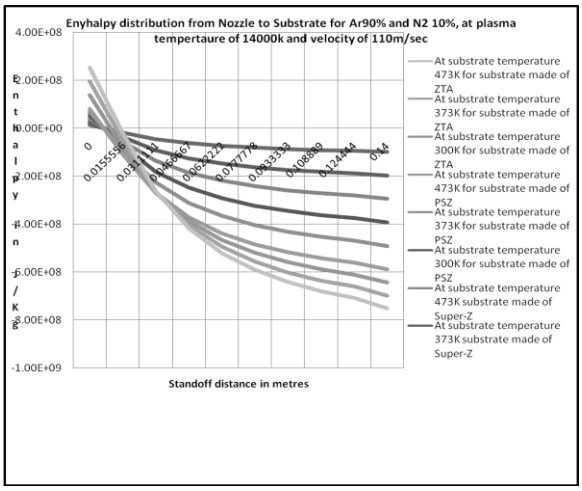

Fig.9.d. Enthalpy distribution for sod =0.14m at 110 m/sec and Ar90%+$N_2$10%.

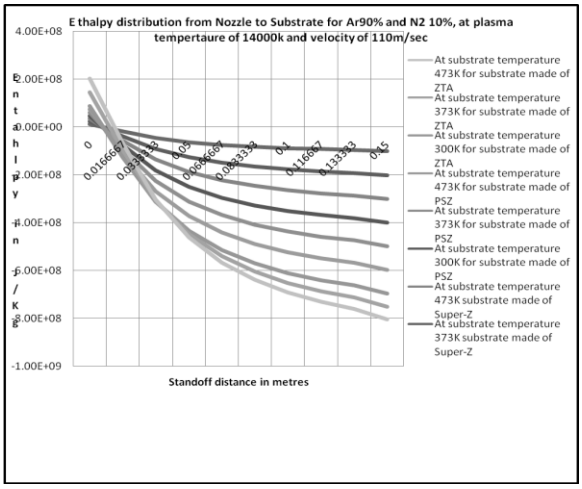

Fig.9.e. Enthalpy distribution for sod =0.15 m at 110m/sec and Ar90%+$N_2$10%.

www.ijmer.com Vol.1, Issue.2, pp-430-442 ISSN: 2249-6645

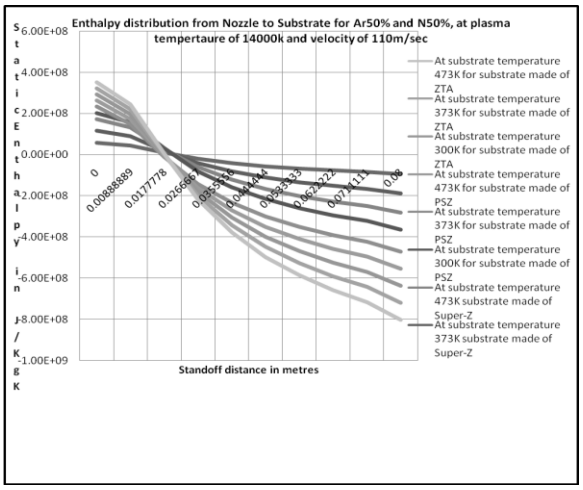

Fig.10.a. Enthalpy distribution for sod =0.08 m at 110 m/sec and Ar50%+$N_2$50%.

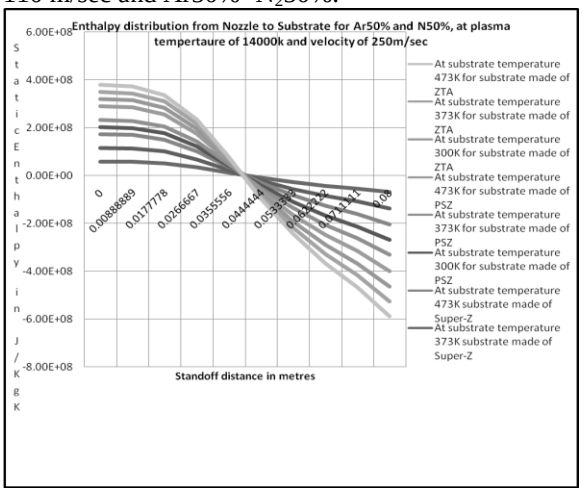

Fig.10.b. Enthalpy distribution for sod =0.08 m at 250 m/sec and Ar50%+$N_2$50%.

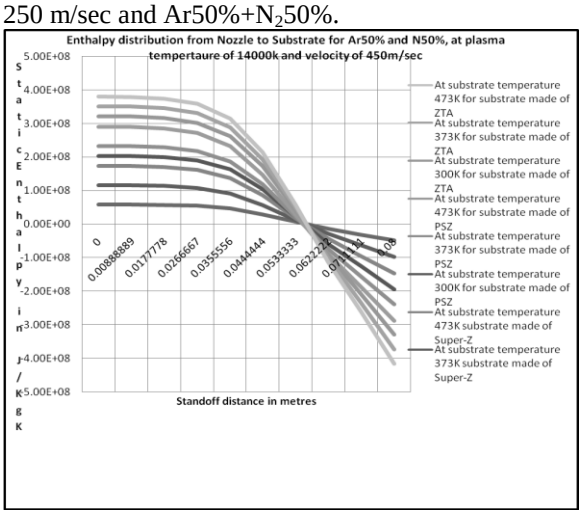

Fig.10.c. Enthalpy distribution for sod =0.08 m at 450m/sec and Ar50%+$N_2$50%.

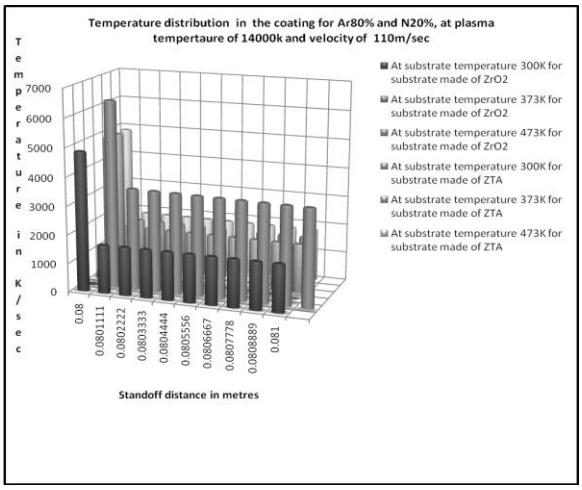

Fig.11.a. Temperature along the thickness of coating for sod =0.08 m at 110 m/sec and Ar50%+$N_2$50%.

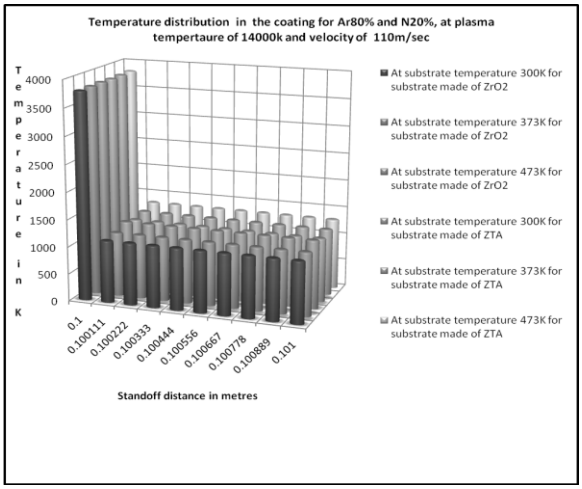

Fig.11.b.Temperature along the thickness of coating for sod =0.10 m at 110 m/sec and Ar50%+$N_2$50%.

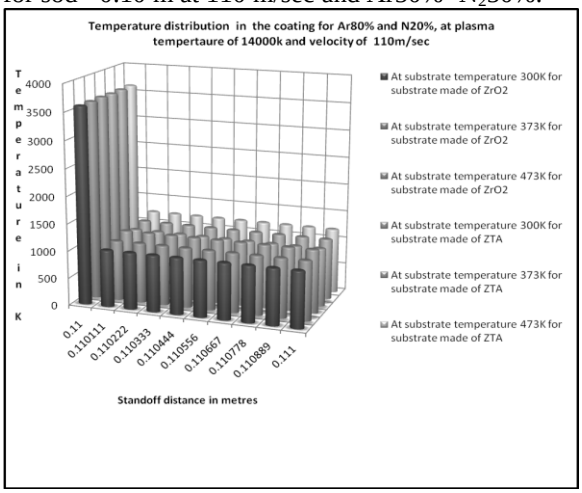

Fig.11.c.Temperature along the thickness of coating for sod =0.11 m at 110 m/sec and Ar 50%+N_2 50%.

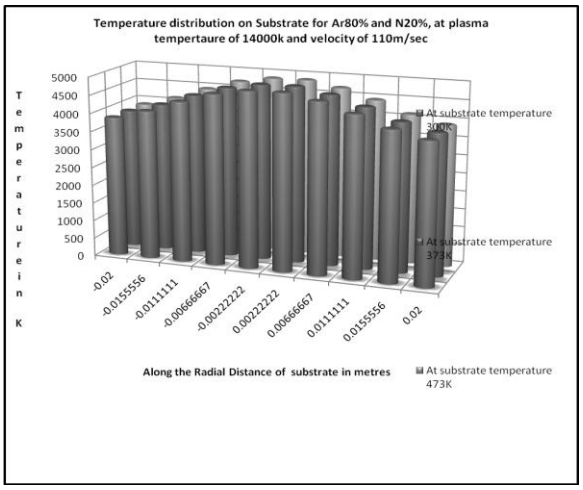

Fig.12.a.Temperature along the radial direction of substrate for sod =0.08 m. at 110 m/sec.

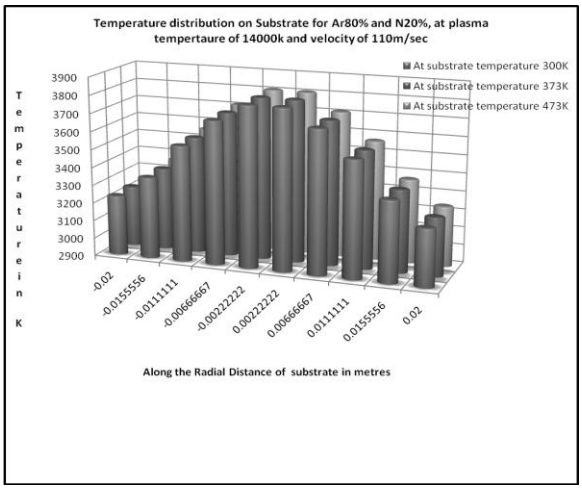

Fig.12.d.Temperature along radial direction of substrate for sod =0.1 m at 110 m/sec.

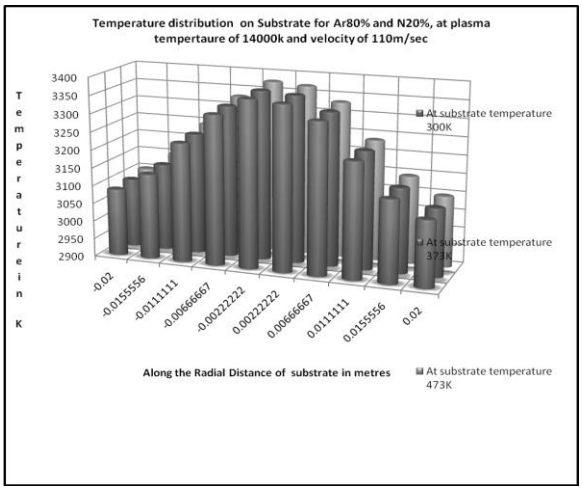

Fig.12.b.Temperature along radial direction of substrate for sod =0.11 m at 110 m/sec.

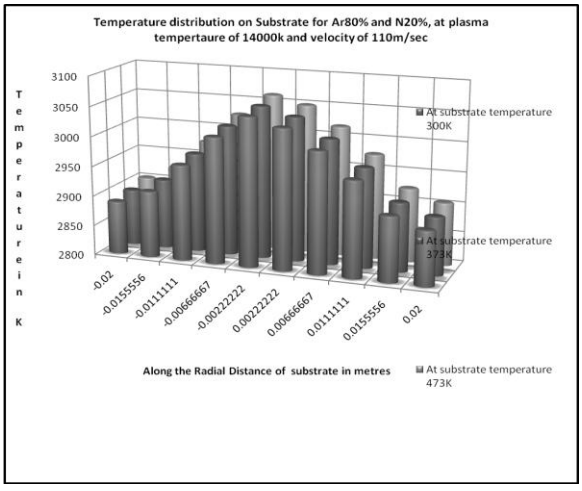

Fig.12.e.Temperature along radial direction of substrate for sod =0.15 m at 110 m/sec.

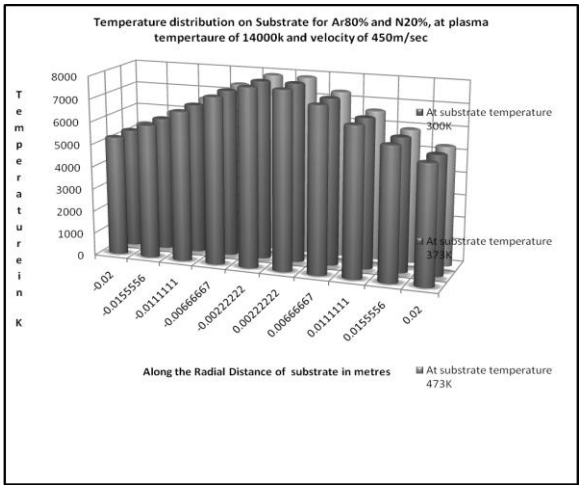

Fig.12.c.Temperature along radial direction of substrate for sod =0.08 m at 450 m/sec.

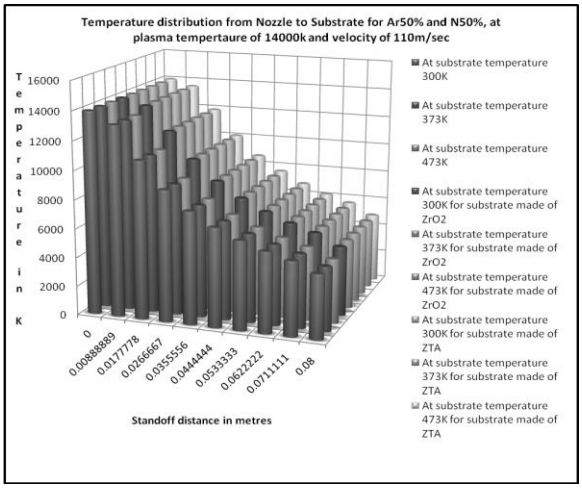

Fig.13.a.Temperature distribution for sod =0.08 m at 110 m/sec and Ar50%+$N_2$50%.

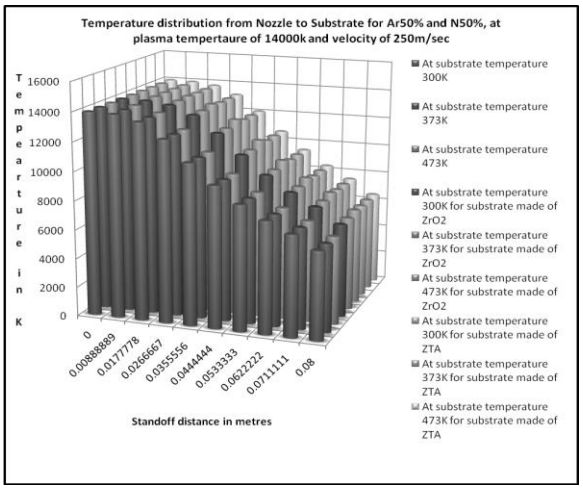

Fig.13.b.Temperature distribution for sod =0.08m at 250 m/sec and Ar50%+$N_2$50%.

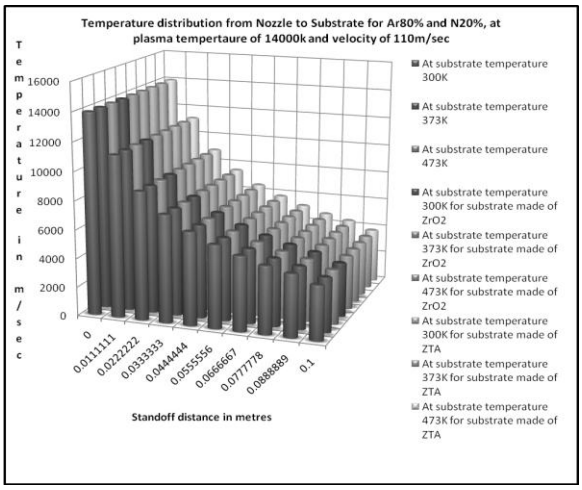

Fig.13.e.Temperature distribution for sod =0.1m at 110 m/sec and Ar80%+$N_2$20%.

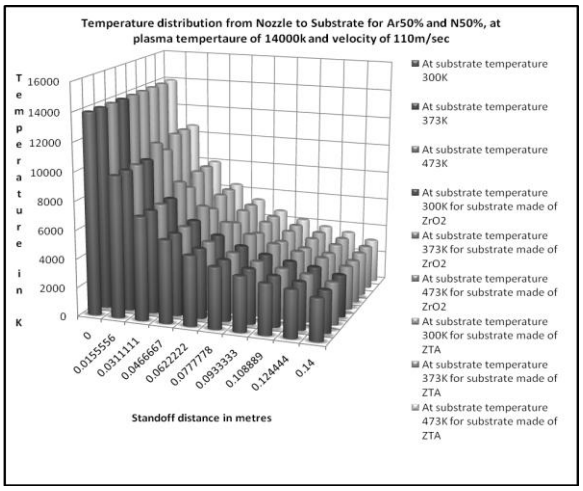

Fig.13.c.Temperature distribution for sod =0.14 m at 110 m/sec and Ar50%+$N_2$50%

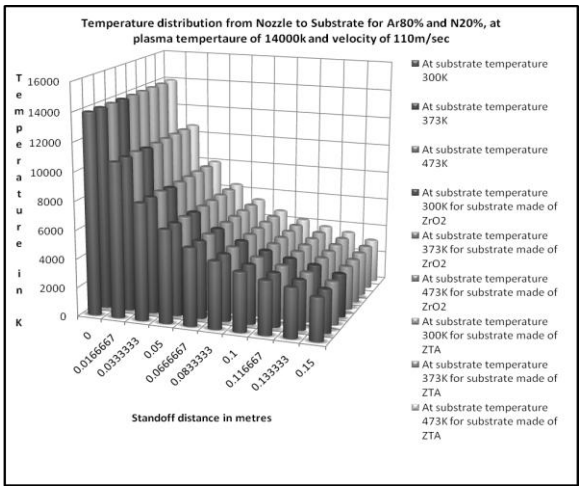

Fig.13.f.Temperature distribution for sod =0.15 m at 110 m/sec and Ar80%+$N_2$20%.

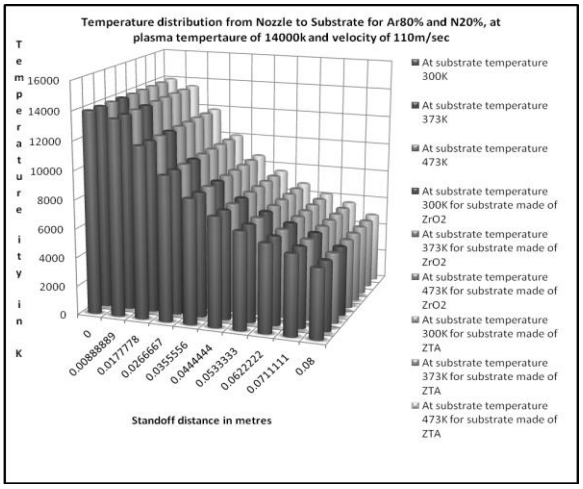

Fig.13.d.Temperature distribution for sod =0.08m at 110 m/sec and Ar80%+N220%.

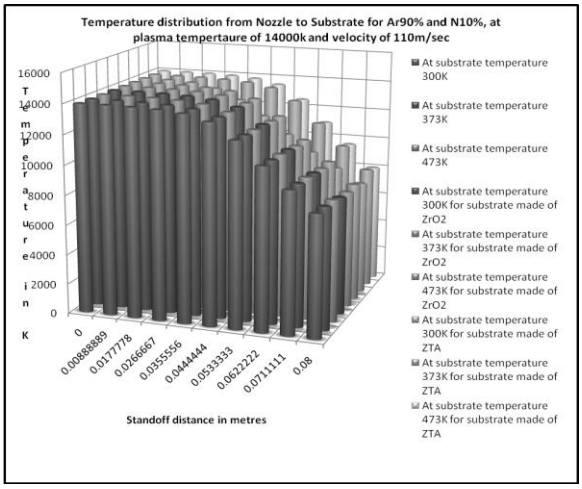

Fig.13.g.Temperature distribution for sod =0.08 m at 110 m/sec and Ar90%+$N_2$10%.

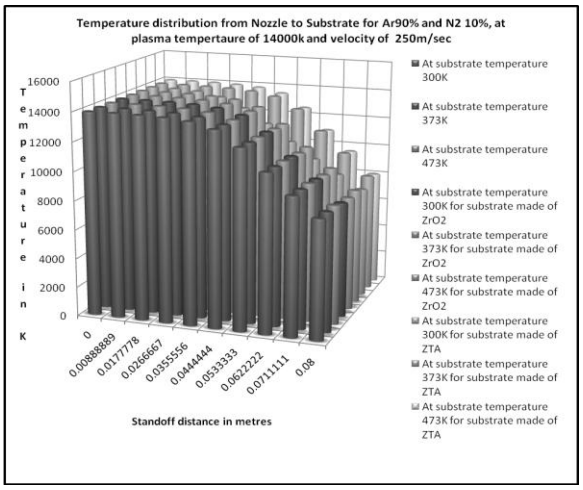

Fig.13.h.Temperature distribution for sod =0.08 m at 250 m/sec and Ar 90%+$N_2$10%.

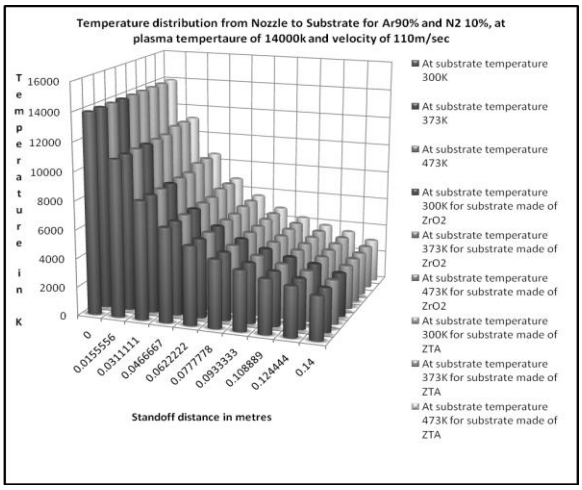

Fig.13.k.Temperature distribution for sod =0.14 m at 110 m/sec and Ar 90%+$N_2$10%.

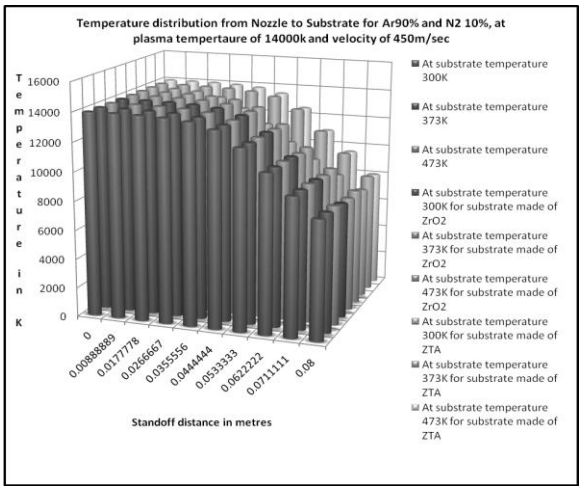

Fig.13.i.Temperature distribution for sod =0.08 m at 450 m/sec and Ar 9 0%+N210%.

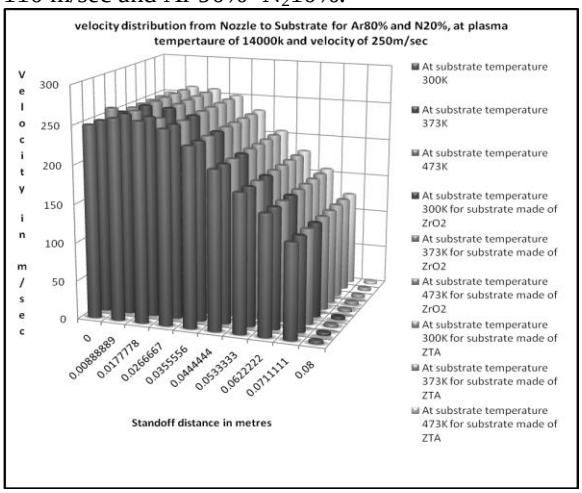

Fig.14.a.Velocity distribution for sod =0.08 m at 250 m/sec and Ar 80%+N220%.

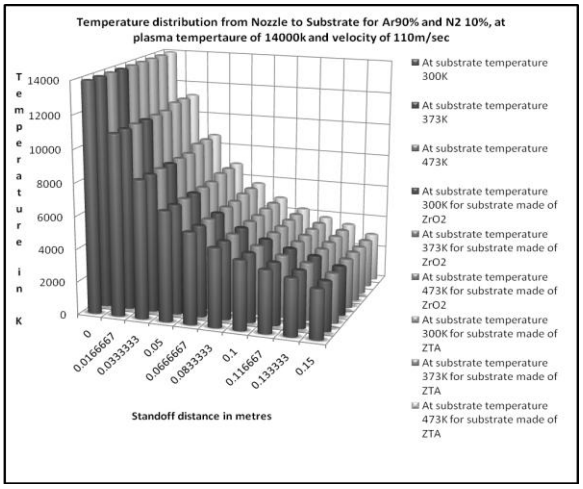

Fig.13.j.Temperature distribution for sod =0.15 m at 110 m/sec and Ar 90%+$N_2$10%.

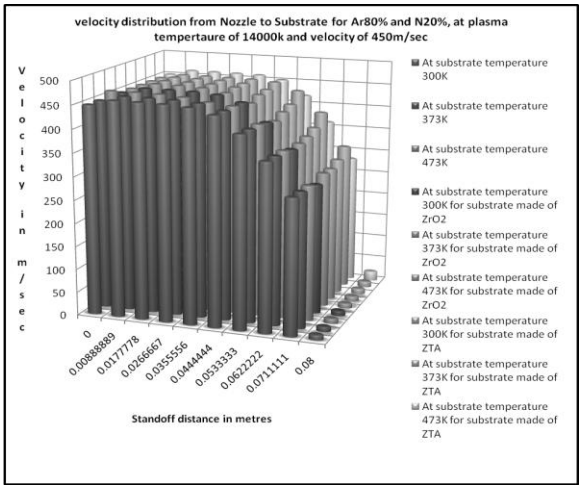

Fig.14.b. Velocity distribution for sod =0.08 m at 450 m/sec and Ar 90%+$N_2$10%.

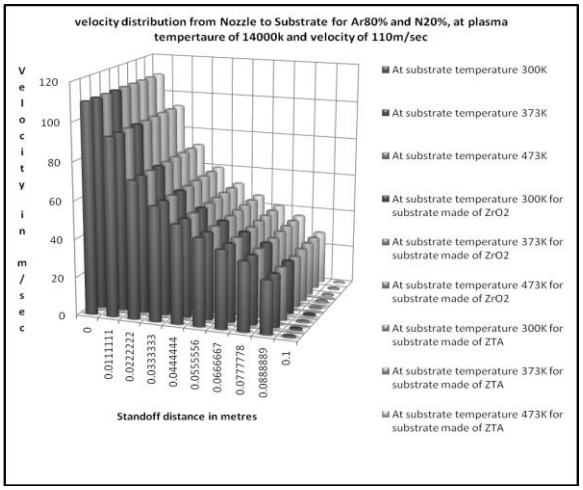

Fig.14.c. Velocity distribution for sod =0.1 m at 110 m/sec and Ar 80%+$N_2$20%.

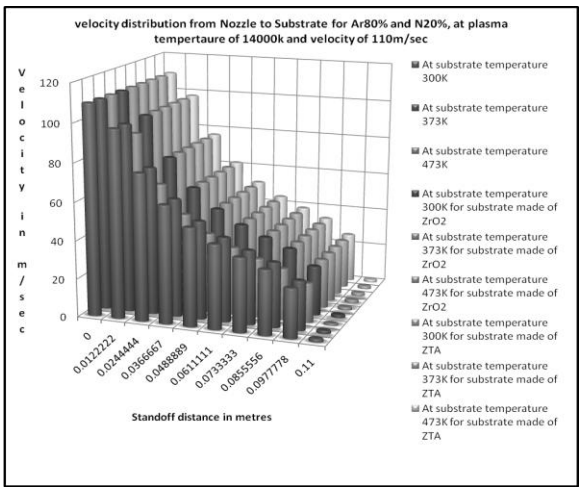

Fig.14.d. Velocity distribution for sod =0.11 m at 110 m/sec and Ar 80%+N220%.

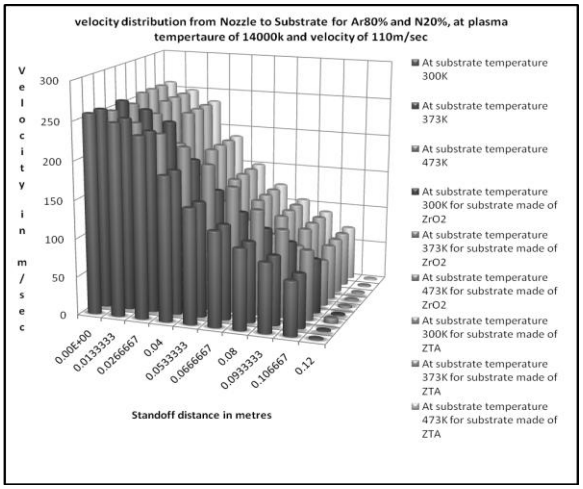

Fig.14.e. Velocity distribution for sod =0.12 m at 110 m/sec and Ar 80%+$N_2$20%.

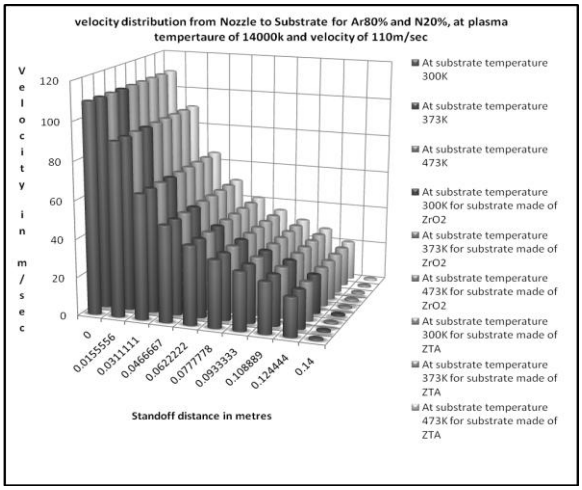

Fig.14.e. Velocity distribution for sod =0.14 m at 110 m/sec and Ar 80%+$N_2$20%.

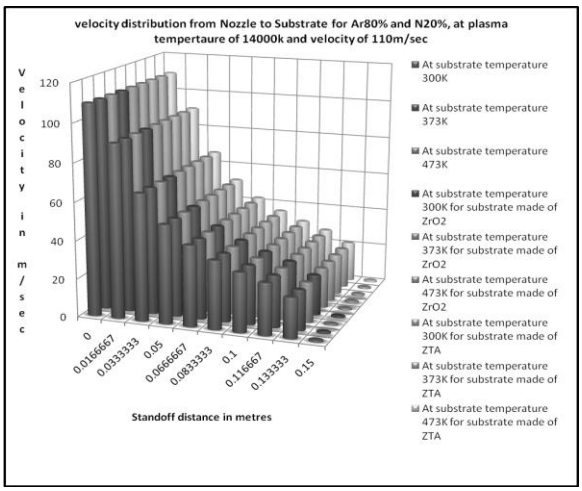

Fig.14.f. Velocity distribution for sod =0.15 m at 110 m/sec and Ar 80%+$N_2$20%.

The effect of gas flow rate on heat flux to the substrate at the stand-off distance of 0.08 m is shown in Fig. 8(a) to 8(e), 9(a) to 9 (e), 10 (a) to 10(c) and, 11(a) to 11 (c). Increasing gas flow rate decreases the heat flux to the substrate. The similar effect has been observed at stand-off distances of 0.1m and 0.15 m. As expected, the temperature observed at the center of the substrate is higher and the temperature is gradually decreasing along both radial and axial directions as shown in fig. 12(a) to 12(e), 13(a) to 13(k). The effect of stand-off distance on the temperature distribution in the substrate is significant. Similar results are obtained for all other cases. With increase in velocity, heat flux (enthalpy) more or less remain constant in case of super-Z, whereas in case

of ZTA and PSZ gradually reduces. Hence at higher velocities, super-Z can be preferred.

Thermo-fluid fields are strongly altered close to the substrate whereas the negligible effect of substrate is seen near the inlet. It is noted that the thermo-fluid fields are not symmetric due to application of the three-dimensional profiles at the inlet. Three-dimensional effect of nozzle exit profiles on the temperature and velocity fields of impinging jets shrinks along the axial directions due to the turbulent mixing of Ar-N_2 plasma with cold air. The similar effects have also been observed for other stand-off distance (0.1 and 0.13 m) as shown in fig. 14(a) to 14(f). For a given velocity with increase in substrate temperature, reduction in enthalpy imparted to substrate is marginal in case of super-Z and gradually increases in PSZ and ZTA as shown in fig. 6(a) to 6(e),. Hence Super-Z is preferred. Hence the order of preference is Super-Z, PSZ and ZTA.

The effect of stand-off distance on heat flux to the substrate at different radial distances for figures shown in 7(a) to 7(e). The heat flux to the substrate decreases with increasing stand-off distance and at the center is stronger and falls along the radial distance. There is no significant effect of stand-off distance on the heat flux to the substrate at the radial distance of 0.3 m. At longer radial distance, the difference between heat fluxes to the substrate reduces. The similar effect has been observed for other cases. Between 90mm to100mm standoff distances, the enthalpy imparted to the substrate gradually reduces upto 90mm and thereafter that is maintained constant upto 30mm. Hence it is inferred the standoff distance for getting good quality of coating between 100mm to 130mm.

The temperature and enthalpy variation along the radial direction of substrate remains more or less constant at standoff distances (less than 90mm) and decreases at increasing standoff distance in general. Reduction is more in case of enthalpy and temperature along radial direction decreases with decrease in substrate temperature. Enthalpy and temperature distribution along coating thickness remains constant at all standoff distances and substrate temperature and velocity of jets (which is because of micro level coating thickness).Marginal change in composition of gas does not have any effect on enthalpy distribution over coating surface remains unaltered.

With increase in percent of Argon in the gas mixture enthalpy imparts to the substrate is comparatively more than at lower compositions of Argon in gas mixture. The temperature obtained at surface coating in respect of super-Z is more compared to ZTA below Standoff distance 90mm and thereafter there is increase in ZTA compared to Super-Z.

3. CONLUSIONS

A three-dimensional numerical model is developed to simulate the Ar-N_2 plasma jet impinging on a flat surface coated with TBC coatings, namely Zirconia Toughened Alumina (ZTA), Partially Stabilized Zirconia (PSZ) and Super-Z. Since the arc root attachment at the anode creates three-dimensional effects both on temperature and velocity of plasma inside the torch, the three-dimensional feature extends to the plasma jet. However, this effect diminishes towards the substrate with different substrate temperatures. Plasma jet velocity is more sensitive to the gas flow rate than temperature especially near the inlet and the effect of gas flow rate on both temperature and velocity of the plasma jet diminishes along the axial direction. The atmospheric condition has strong influence on the heat transfer (rate of heat energy transfer through a given surface) between the plasma jet and the substrate. The effect of gas flow rate on the heat flux to the substrate decreases with decreasing the gas flow rate. The stand-off distance strongly controls the heat flux to the substrate at the center and is loosing its control on the heat flux to the substrate along the radial direction. The stand-off distance strongly influences the temperature distribution in the substrate. Modeling has been done with respect to above three coatings and for good quality of coating, the optimization of various process parameters has been done. This study is useful to understand the thermal exchange between the plasma jet and the substrate which decides the selection of TBC and optimization of process parameters for the production of a given surface condition based on engineering requirement.

REFERENCES

[1] Dr.J.Fazlur rahman and Mohammed Yunus, "Benefits of TBC Coatings on Engine applications", in *Proc. International conference, INCAM,* 2009 at Kalsalingam University, Tamil Nadu.

[2] R. Bolot, M. Imbert, and C. Coddet, "Use of a Low-Reynolds Extension to the Chen-Kim(k-ε) Model to Predict Thermal Exchanges in the Case of an Impinging Plasma Jet", *Int. J. Heat Mass Transfer, 44,* 2001, pp.1095-1106.

[3] Dr.J.Fazlur rahman and Mohammed Yunus, "Study of Mechanical and Tribological Characteristics of Tungsten Carbide-Cobalt HVOF Coating", *Proc. International conference, MEMS,* 2008 at AEC Bhatkal, Karnataka.

[4] Dr.J.Fazlur rahman and Mohammed Yunus, "Micro wave irradiation effect on ceramic composite coatings and carbide cutting tools", *Proc. National conference and proceedings, FTME- 2010,* at Gurunanak Dev college of Engineering, Ludhiana, Punjab.

[5] H.P. Li and E. Pfender, "Three Dimensional Modeling of the Plasma Spray Process", *J. Thermal Spray Technology, 16,* 2007, pp. 245-260.

[6] A.B. Murphy, "Transport Coefficients of Air, Argon-Air, Nitrogen-Air, and Oxygen-Air Plasmas" *Plasma Chem. Plasma Process.*, 1995, 15, pp. 279-307.

[7] Numerical Modelling of Ar-N_2 Plasma Jet Impinging on a Flat Substrate by B. Selvan, K. Ramachandran, B. C. Pillai and D. Subhakar *Journal of Thermal Spray Technology* ASM International, 2010.

[8] K.A. Khor, S. Jana, Pulse laser processing of plasma sprayed thermal barrier coating, *Journal of Materials Processing Technology, 66,* 1996, pp. 4-8.

[9] A.K. Ray, Characterization of bond coat in a thermal barrier coated super alloy used in combustor liners of aero engines, *conference in Materials Characterization 57,* 2006, pp. 199-209.

[10]G. Moskal, L. Swadźba, T. Rzychoń, "Measurement of residual stress in plasma-sprayed TBC with a gradient of porosity and chemical composition, *Journal of Achievements in Materials and Manufacturing Engineering, 23, 2,* 2007, pp. 31-34.

[11]Gorlach, I.A. High Velocity Thermal Gun for Surface\Preparation and Treatment, *South African Journal for Industrial Engineering,13, 1,* 2002, pp. 131 –143.

[12] Verstak, A., Baranovski, V. - *AC-HVAF Sprayed Tungsten Carbide: Properties and Applications*, *Proceedings of the International Thermal Spray Conference*, Seattle, Washington, USA, 2006.

[13]DeMasi, J.T., Sheffler K.D. and Ortiz M., 1989, "Thermal Barrier Coating Life Prediction Model Development," Phase-I, *Proc. Life Prediction of Functionally Graded Thermal Barrier Coatings*, 1989, NASA-182230.

[14] Xi Chen a, John W. Hutchinson , Anthony Evans G. "Simulation of the high temperature impression of thermal barrier coatings with columnar microstructure", *Journal of Acta Materialia, 52*, 2004, pp. 565–571.

[15] K. Ramachandran, N. Kikukawa, and H. Nishiyama, 3D Modeling of Plasma-Particle Interactions in a Plasma Jet Under Dense Loading Conditions, *Journal of Thin Solid Films, 435,* 2003, pp.298-306.

[16] B. Selvan, K. Ramachandran, K.P. Sreekumar, T.K. Thiyagarajan, and P.V. Ananthapadmanabhan, Three-Dimensional Numerical Modeling of an Ar-N_2 Plasma Arc Inside a Non-Transferred Torch, *Plasma Science Technology*, 2009, 11,pp.679-687.

[17] H. Fukanuma, R. Huang, Y. Tanaka, and Y. Uesugi, Mathematical Modeling and Numerical Simulation of Splat Cooling in Plasma Spray Coatings, *Journal of Thermal Spray Technology,* 2009,18, pp.965-974.

[18] H.R. Salimijazi, L. Pershin, T.W. Coyle, J. Mostaghimi, S. Chandra, Y.C. Lau, L. Rosenzweig, and E. Moran, Effect of Droplet Characteristics and Substrate Surface Topography on the Final Morphology of Plasma-Sprayed Zirconia Single Splats, *Journal of Thermal Spray Technology*, 2007, 16, pp. 291-299.

[19] Mohammed yunus, Dr.J. Fazlur rahman, "optimization of usage parameters of ceramic coatings in high temperature applications using Taguchi design" *International Journal of Engineering science and Technology, Vol.3(8),* 2011, pp.193-198.